 CMES, vol.85, no.6, pp.521-541, 2012

The Self-Alignment of Microparts in Solutions

Tsung-Yu Huang[1] **and Wen-Hwa Chen**[1,2]

Abstract: A rigorous three-dimensional analysis model is established to calculate the restoring force and restoring torque for the self-alignment of the micropart with the binding site in solution using the Surface Evolver Program, which is developed for analyzing the liquid formation due to surface tension and other energies. The motions of the micropart studied include translation, compression, yawing and rolling, respectively.

To improve the drawbacks of the simplified models reported in the literature, the effects of the buoyancy and hydrostatic pressure on the micropart and the hydrostatic pressure on the lubricant droplet between the micropart and binding site are explored. The deformation and contact characteristics of the lubricant droplet between the micropart and binding site in solution are therefore elucidated accurately in the present analysis model. Besides, the critical values of the restoring force and restoring torque, which indicate the capability of the self-alignment of the micropart, are calculated for various volumes of lubricant droplets in different solutions, respectively. It is found that the self-alignment of the micropart in water is better than that in ethylene glycol solution and air, and the self-alignment under translation and rolling should receive more attentions.

Keywords: Self-alignment, Interfacial Tension, Restoring Force, Restoring Torque, Fluidic Self-assembly Technique.

1 Introduction

The development of an accurate and efficient assembly technique in micro-electromechanical systems has attracted considerable interest in recent years (Elwenspoek *et al.*, 2010). The fluidic self-assembly technique (Talghader, 1998) utilizes solution to make microparts touch with lubricant droplets placed on the surfaces of binding sites, as seen in Fig.1. The micropart is subjected to interfacial tension

[1] Dep. of Power Mech. Engng., National Tsing Hua University, Hsinchu, Taiwan, R.O.C.
[2] Corresponding Author

or capillary force to align with the binding site. This technique has numerous advantages over the traditional pick-and-place assembly - the increased accuracy and efficiency of the self-alignment of the micropart with the binding site, the promoted filling of holes using recirculation systems and the robust assembly of thousands to millions of similar devices in parallel, etc. (Lienemann *et al*., 2003).

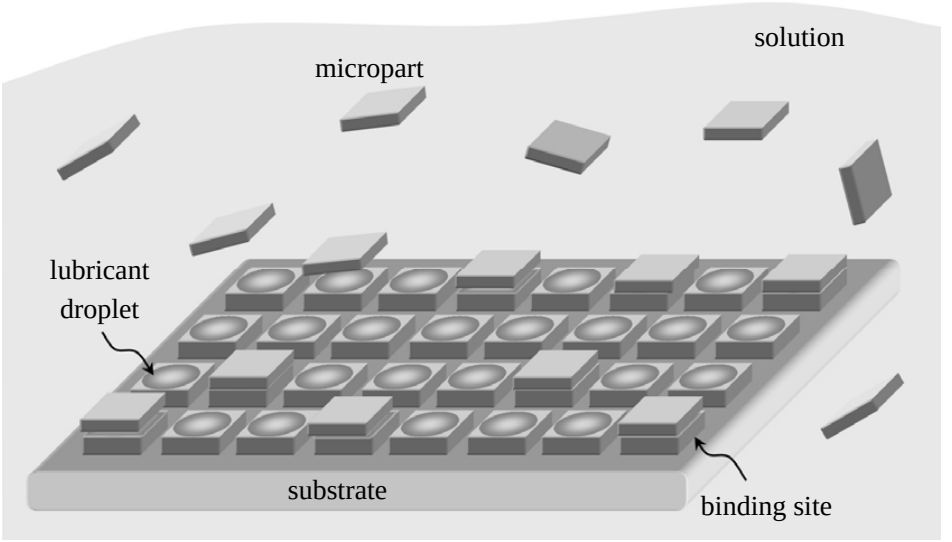

Figure 1: The self-alignment of microparts with binding sites in solution

Sato *et al.* (1999, 2003) investigated the self-alignment of various geometric shapes of microparts with a binding site in air by a precise experiment. The hexagonal micropart yielded a smaller alignment error than the other shapes. Further, the overflow of a droplet close to the sides of the micropart and binding site and the non wetted area in the corners of the micropart and binding site were observed in the experiment. Srinivasan *et al.* (2001) performed the self-alignment experiment on different shapes of microparts with a binding site using the hexadecane lubricant droplet in water. The approximately circular and square microparts provided a good alignment precision than those of the other shapes. Mastrangeli *et al.* (2010) practiced an experiment on the self-alignment of a circular micropart with a corresponding binding site. The conceptually simple experimental setup was designed when the micropart underwent translation. Takei *et al*. (2010) explored the self-alignment experiment on the rotation of the microparts with various shapes. It was noted that the gravity of the microparts and the height of the droplets affected the

measured torque tremendously.

Numerous of the self-alignment of a micropart with a binding site in air has involved simulations using the Surface Evolver Program (Brakke, 1996). Xie *et al*. (2007) utilized the surface tension and contact angle to investigate the formation of the droplet. Zhu *et al.* (1998) estimated the restoring force that was caused by the misalignment for various sizes of solder volume, bump and solder pad. Kim *et al.* (2004, 2005) computed the restoring force of the micropart under translation for different droplets, such as resin droplet and molten solder droplet. It was found that the self-alignment, even when using the resin droplet with lower surface tension, will behave precisely. Berthier *et al.* (2010) investigated the restoring force, restoring torque and total potential energy when the micropart was caused by different volumes of droplets under various motions. The size of droplet volume studied is from 250nl to 2500nl. Chen and Huang (2010) predicted the critical restoring force and restoring torque when the micropart underwent similar motions for much smaller droplets with the volume about 12nl to 35nl. The contact characteristics between the micropart and the binding site was also explored elaborately.

Several studies have adopted the Surface Evolver Program to simulate the self-alignment of a micropart with a binding site in solution. Lienemann *et al*. (2002) evaluated the restoring force and restoring torque of the micropart under translation and yawing for various interfacial tensions between the lubricant droplet and the solution by a simplified model ignoring the effects of buoyancy and hydrostatic pressure on the micropart and hydrostatic pressure on the lubricant droplet. By the same model, Greiner *et al*. (2002) calculated the restoring force and restoring torque when the micropart underwent the same motions in water for various volumes of hexadecane lubricant droplets. Unfortunately, due to the lack of the geometry and material data of the micropart in those works (Lienemann *et al*., 2002; Greiner *et al*., 2002), it is not feasible to verify their results obtained. Lu *et al*. (2006) employed the similar model to elucidate the deformation of the hexadecane lubricant droplet in water. It was found that the restoring force increases with the translation of the micropart.

To improve the drawbacks of those works (Lienemann *et al*., 2002; Greiner *et al*., 2002; Lu *et al*., 2006), this work is thus to use the Surface Evolver Program to analyze the self-alignment of the micropart with the binding site for various volumes of lubricant droplets in different solutions, considering the buoyancy and hydrostatic pressure on the micropart and the hydrostatic pressure on the lubricant droplet. In fact, in the implementation of fluidic self-assembly technique, the micropart may move arbitrarily and contact the lubricant droplet in solution from any possible directions. The motion of the micropart can be viewed as a combination of translation, compression, yawing and rolling. Thus, for practical application, the

self-alignment of the micropart should have an over-all evaluation for all motions. In addition, the critical values of the restoring force and restoring torque are also estimated. The changes in the contact line and the wetted area among the micropart, binding site, lubricant droplet and solution are also drawn thoroughly. The results achieved will increase the precision of the self-alignment of microparts in solutions and will be helpful for the future development of fluidic self-assembly technique.

2 Effects of Buoyancy and Hydrostatic Pressure

The deformation of the lubricant droplet between the micropart and the binding site in solution is influenced by the interactions of the gravity, buoyancy, hydrostatic pressure and interfacial tensions (γ_{ds}, γ_{dm}, γ_{db}, γ_{ms} and γ_{bs}) at the interfaces of lubricant droplet and solution S_{ds}, lubricant droplet and micropart S_{dm}, lubricant droplet and binding site S_{db}, micropart and solution S_{ms} and binding site and solution S_{bs}, respectively. As seen in Fig. 2, the micropart may undergo a motion combined by translation Δx, compression Δz, yawing $\Delta\phi_1$ and rolling motion $\Delta\phi_2$. Neglecting the inertial effects of viscosity and hydrodynamic interactions (Chen *et al.*, 2005), a quasi-static analysis is adopted herein.

The present analysis model for the self-alignment of the micropart with the binding site in solution is presented in Fig. 3. By placing a hexadecane lubricant droplet under a shallow surface of water, Böhringer's experiment (Böhringer *et al.,* 2001) showed that the interfacial tensions (γ_{ds}, γ_{dm}/γ_{db} and γ_{ms}/γ_{bs}) loaded at the corresponding interfaces (S_{ds}, S_{dm}/S_{db} and S_{ms}/S_{bs}) were 52.2, 1 and 46 dynes/cm, respectively. By the Lu's simplified model (Lu *et al.*, 2006), in addition to the interfacial tensions (γ_{ds}, γ_{dm}/γ_{db} and γ_{ms}/γ_{bs}), the additional external loadings applied included the total gravity of the micropart and the hexadecane lubricant droplet G, and the buoyancy of the hexadecane lubricant droplet B_d. However, the buoyancy of the micropart B_m and the hydrostatic pressures P_m and P_d exerted on the micropart and hexadecane lubricant droplet were not accounted for and should be cautiously considered. In addition, it is worthwhile to mention that the interfacial tensions γ_{ds} and γ_{ms}/γ_{bs} at the interfaces S_{ds} and S_{ms}/S_{bs} were mistakenly placed each other in the Lu's work and corrected in this work.

To accurately explore the deformation of the hexadecane lubricant droplet in solution and the contact behaviors among the hexadecane lubricant droplet, solution, micropart and binding site, a rigorous three-dimensional analysis model is established and can be viewed in Fig. 3. In addition to the gravity of the micropart and the hexadecane lubricant droplet G and the buoyancy of the hexadecane lubricant droplet B_d, the hydrostatic pressure exerted on the hexadecane lubricant droplet P_d, the buoyancy B_m and the hydrostatic pressure P_m caused by the micropart are also considered, while the same interfacial tensions (γ_{ds}, γ_{dm}/γ_{db} and γ_{ms}/γ_{bs}) are loaded

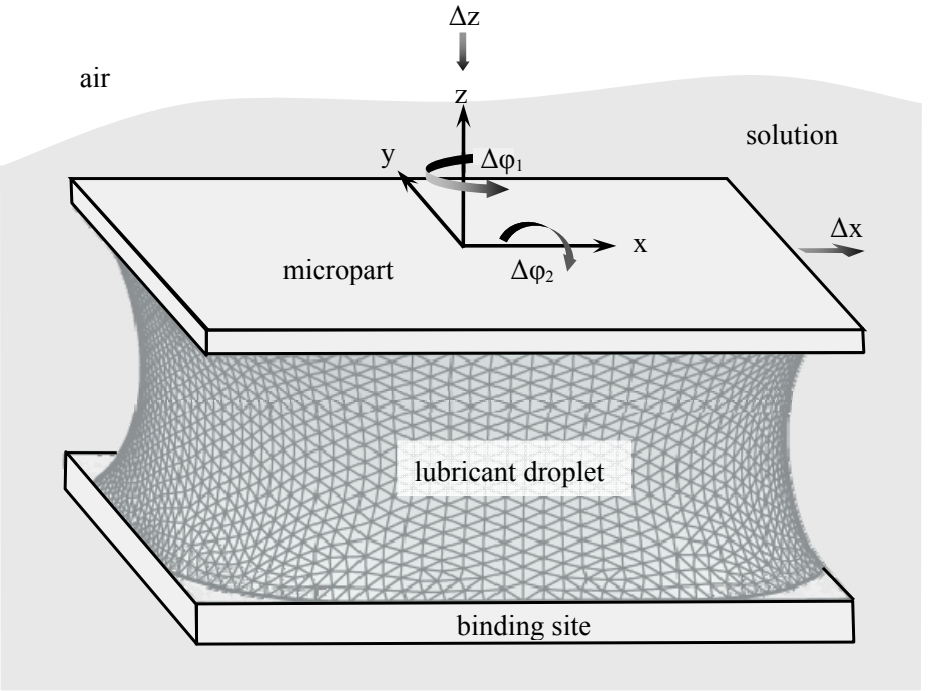

Figure 2: The motions of the micropart in solution

at the interfaces S_{ds}, S_{dm}/S_{db} and S_{ms}/S_{bs}, respectively. Besides, the self-alignment for the micropart is assumed to be undertaken under 3cm depth from the surface of solution (Srinivasan *et al.*, 2001).

3 Implementation of Surface Evolver Program

The Surface Evolver Program utilizes iterative calculation to study the formation of the droplet shaped by the effect of the total energy composed of surface tension and other energies. In dealing with the surface of the droplet, the Surface Evolver Program initially subdivides its surface into many small triangular facets, and then regularizes the position of each vertex and area of the small triangular facet, and evolves the total energy toward its minimum by a gradient descent method (Cabestany *et al.*, 2011). In addition to tackle the surface of droplet, the Surface Evolver Program can also handle the constraints of the problem appropriately, such as the prescribed volume of the droplet and the complex external boundaries, etc.

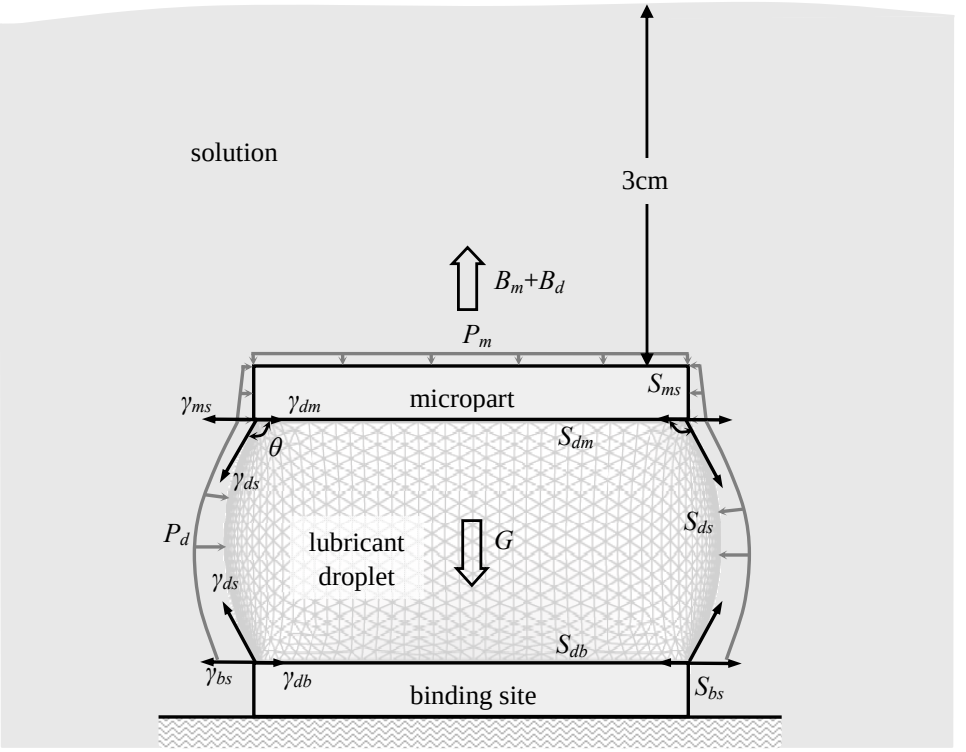

Figure 3: The present analysis model for the self-alignment of the micropart with the binding site in solution

As calculated by the Surface Evolver Program, there are three types of integrals involved, say, (1) surface integral, (2) plane integral and (3) volume integral. In general, the energies from the surface tension are calculated by the surface integral. The energies occurred at the plane are computed by the plane integral, which can be transformed to line integrals by the Stokes' theorem (Zill and Cullen, 2000). Furthermore, the volume integral is applied to calculate the energies due to the gravity and buoyancy, which can be transformed to surface integrals by the divergence theorem (Zill and Cullen, 2000). Such implementations are helpful in controlling the contact angles of the droplet on the plane (Brakke, 1992).

In this work, based on the minimization of the total energy, the Surface Evolver Program is adopted to evolve the deformation of the lubricant droplet between the micropart and binding site in solution. By the present analysis model, the total

energy E_{total} is composed of the energy induced by surface tension $E_{surface\ tension}$, the energy due to gravity $E_{gravity}$, the energy due to buoyancy $E_{buoyancy}$ and the energy due to pressure $E_{pressure}$, say,

$$E_{total} = E_{surface\ tension} + E_{pressure} + E_{gravity} + E_{buoyancy}\ . \tag{1}$$

In the above,

$$E_{surface\ tension} = \int_{S_{ds}} \gamma_{ds} dA + \int_{S_{dm}} \gamma_{dm} dA + \int_{S_{db}} \gamma_{db} dA + \int_{S_{ms}} \gamma_{ms} dA + \int_{S_{bs}} \gamma_{bs} dA, \tag{2}$$

$$E_{pressure} = \int \left(\int_{S_{ds}} P_d dA \right) dr + \int \left(\int_{S_{ms}} P_m dA \right) dr, \tag{3}$$

$$E_{gravity} = \int_{\Omega_d} (-\rho_d g z)\ dV + \int_{\Omega_m} (-\rho_m g z)\ dV + \int_{\Omega s} (-\rho_s g z)\ dV, \tag{4}$$

and

$$E_{buoyancy} = \int \left(\int_{\Omega_d} \rho_s g dV \right) dz + \int \left(\int_{\Omega_m} \rho_s g dV \right) dz, \tag{5}$$

where (Ω_d, ρ_d), (Ω_m, ρ_m) and (Ω_s, ρ_s) denote the volumes and densities of the lubricant droplet, micropart and solution, respectively; dr is a tiny displacement along the normal direction of the interfacial surfaces S_{ds} and S_{ms}. As mentioned above, three types of integrals involved from Eqs. (2) to (5). The first type of surface integral is used to compute the energies through the smooth surface of the lubricant droplet discretized by triangular facets, as shown in the first terms of Eqs. (2) and (3). The second type of plane integral deals with the computation of the energies occurred at the interfacial planes S_{dm}, S_{db}, S_{ms} and S_{bs}, as appeared in the other terms of Eqs. (2) and (3). The third type of volume integral is adopted to calculate the energies induced from the gravity and buoyancy, as shown in Eqs. (4) and (5). The negative symbol "–" in Eq.(4) represents the downward direction of the gravity for each triangular facet as referred to the coordinate system shown in Fig. 2. A sufficient domain Ω_s of the solution is provided such that the boundary effect can be avoided.

It is noted that the vertices, edges and facets, discretized from the lubricant droplet, micropart, binding site and solution at the interfacial planes S_{ds}, S_{dm}, S_{db}, S_{ms} and S_{bs}, can be concurrent, collinear and coplanar. To depict the distribution of the contact line and the wetted area distinctly, the corners of the interface planes S_{dm}, S_{db}, S_{ms} and S_{bs} and the interface surface between the lubricant droplet and solution

S_{ds} are suggested to subdivide into much more refined facets. For example, the former regions are subdivided into 35,177 facets and the latter one with 13,927 facets, as compared with the micropart and binding site with 48 basic facets.

When the micropart undergoes an increment of motion (Δx, Δy, Δz, $\Delta\phi_1$ or $\Delta\phi_2$), the restoring force (F_x, F_y or F_z) and the restoring torque τ can be computed by the partial derivatives of the total energy E_{total} accordingly. For example, the horizontal restoring force F_x is computed by

$$F_x = \frac{\partial E_{total}}{\partial x} \approx \frac{\Delta E_{total}}{\Delta x}, \tag{6}$$

and the restoring torque τ is calculated as

$$\tau = \frac{\partial E_{total}}{\partial \phi} \approx \frac{\Delta E_{total}}{\Delta \phi} \quad . \tag{7}$$

The increment of motions selected will affect the computed accuracy of the self-alignment of the micropart. The increment of motions taken should be small enough. Otherwise, the contact line may move away from the side of the micropart and the lubricant droplet cannot rewet the micropart. This will strongly alter the self-alignment of the micropart. The increment of translation and compression adopted in this work is 0.01μm, and that of yawing and rolling is 0.01°.

4 Results and Discussion

By the present model established, the self-alignment of the micropart with the binding site for various volumes of lubricant droplets in different solutions is analyzed herein. The restoring force and restoring torque, together with their critical values, induced on the micropart in solutions under translation, compression, yawing and rolling are computed, respectively.

4.1 The present analysis model

For comparison purpose, the self-alignment of the micropart under a translation Δx in water, as studied by Lu *et al.* (2006), is first analyzed by the present analysis model. The area of the micropart and binding site is taken the same size as that of Lu's work (Lu *et al.*, 2006), say, $1000\times1000\mu\text{m}^2$, with thickness 15μm and density 1.1g/cm^3. The hexadecane lubricant droplet with volume 20nl is placed between the micropart and the binding site. The static height z_0 of the hexadecane lubricant droplet is computed as 19.92μm when the micropart falls in water.

The computed horizontal restoring force F_x induced on the micropart versus the translation Δx of the micropart in water is shown in Fig. 4. The dashed line represents the calculation by Lu *et al.* (2006). The long-short dashed line is the

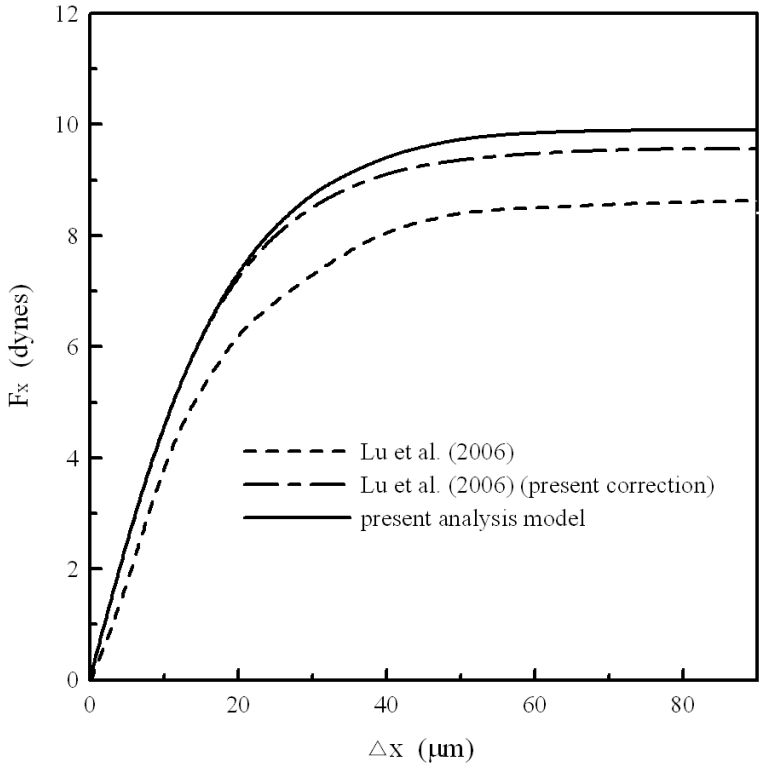

Figure 4: The computed horizontal restoring force F_x versus the translation Δx of the micropart in water

present computed results by the Lu's simplified model after correcting the mistakenly placed interfacial tensions γ_{ds} and γ_{ms}/γ_{bs}. The solid line shows the horizontal restoring force F_x computed by the present analysis model. As displayed in Fig. 4, all calculations of the horizontal restoring force F_x of the micropart increase with the translations Δx. When the translation Δx is less than around 18.7μm, the horizontal restoring force F_x obtained by the present analysis model does not differ from that by the corrected Lu's simplified model. As the translation Δx exceeds about 18.7μm, however, the combined effects of the buoyancy and hydrostatic pressure exerted on the micropart and the hydrostatic pressure on the hexadecane lubricant droplet can be viewed by the present analysis model.

4.2 The self-alignment of microparts in different solutions

To estimate the effect of different solutions on the self-alignment of the micropart with the binding site, in addition to air, two often used solutions, water and 40% ethylene glycol in water, are adopted (Saeedi *et al.*, 2007; Morris and Parviz, 2008; Mastrangeli *et al.*, 2011). The density of ethylene glycol solution is 1.047 g/cm^3. The same sizes of the square micropart and binding site are also taken for study.

The tetradecane lubricant droplet with different volumes of 10nl, 20nl and 40nl is chosen for analysis due to the availability of its interfacial tensions in solutions to deal with. The interfacial tension γ_{ds} between the tetradecane lubricant droplet and the ethylene glycol solution (water) is found as 33.8 dynes/cm (50.2 dynes/cm), while the interfacial tension γ_{ms} (γ_{bs}) between the micropart (binding site) and the ethylene glycol solution is 29.26 dynes/cm. The surface tension of the tetradecane lubricant droplet is 26.5 dynes/cm, and the interfacial tension γ_{dm} (γ_{db}) between the tetradecane lubricant droplet and the micropart (binding site) is less than 1 dynes/cm (Inaba and Sato, 1996; Yang *et al.*, 2003; Karniadakis *et al.*, 2005; Neumann *et al.*, 2011).

The static heights z_0 computed in air are 9.99μm, 19.98μm and 39.96μm for the tetradecane lubricant droplet with volumes of 10nl, 20nl and 40nl, respectively. It is worthwhile to mention that the influence of the solution (air, ethylene glycol solution or water) used on the calculation of the static height z_0 can be ignored.

4.2.1 Translation

Based on the present analysis model, this work further investigates the influence of different solutions with different volumes of lubricant droplets on the self-alignment of the micropart under translation. Fig. 5 shows the present computed horizontal restoring force F_x versus the translation Δx of the micropart in air, ethylene glycol solution and water for various volumes of tetradecane lubricant droplets, respectively. As seen in Fig. 5, the dashed lines represent the computed horizontal restoring force F_x versus the translation Δx in air, the long-short dashed lines show that in ethylene glycol solution and that in water is indicated by the solid lines. The respective computation reveals that the maximum or critical horizontal restoring forces occur at the critical translations Δx_c (30.9μm, 49.1μm and 115.1μm), (44.2μm, 85.1μm and 186.3μm) and (47.7μm, 94.6μm and 210.5μm), for different volumes of the tetradecane lubricant droplets in air, ethylene glycol solution and water.

As displayed in Fig. 5, it is noted that the horizontal restoring force F_x computed by the same volume of the tetradecane lubricant droplet in water is larger than that in ethylene glycol solution and then in air. The critical translation Δx_c increases

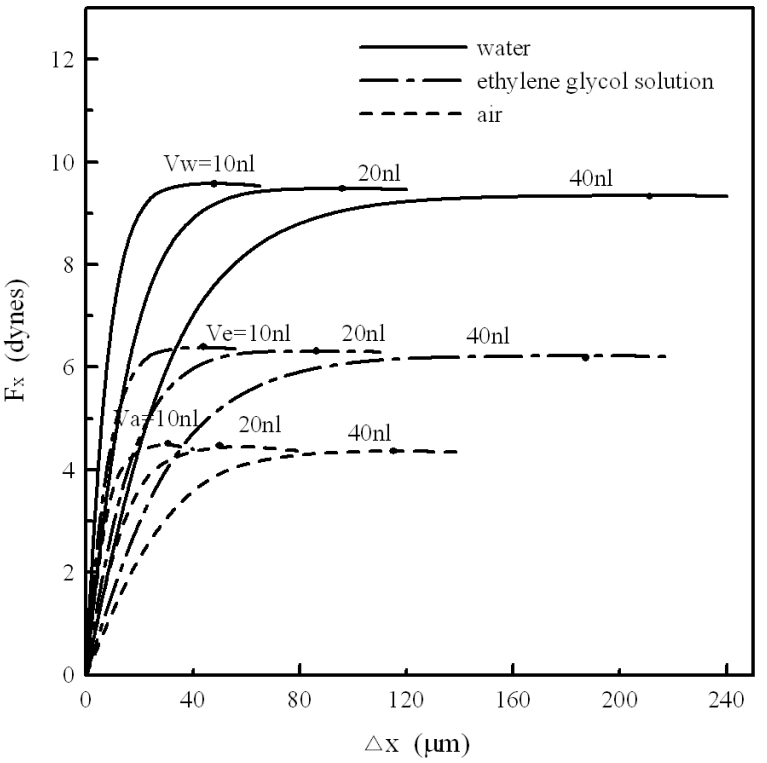

Figure 5: The computed horizontal restoring force F_x versus the translation Δx of the micropart for various volumes of tetradecane lubricant droplets in different solutions

with the volume of the tetradecane lubricant droplet. When the micropart translates less than its critical translation Δx_c, the micropart will self-align to its initial place as the translation Δx is removed. As the translation Δx of the micropart exceeds its critical translation Δx_c, however, the self-alignment of the micropart is altered. Further, as would be expected, the horizontal restoring force increases moderately with the translation Δx for larger volume of the tetradecane lubricant droplet. As demonstrated in Table 1, the critical translations Δx_c for the tetradecane lubricant droplet in water are also greater than those in ethylene glycol solution and air. Hence, among those three situations, the best capability for the self-alignment of the micropart under translation is performed in water, the second is in ethylene glycol solution and the worst is in air.

The shape of the contact line and the wetted area among the micropart, binding site,

Table 1: The critical movements for various volumes of the tetradecane lubricant droplets in solutions

V (nl)	droplet	Δx_c (μm)	Δz_c (μm)	$\Delta\phi_{1c}$ ($^\circ$)	$\Delta\phi_{2c}$ ($^\circ$)
10	air	30.9	0.13	4.68	1.1
	ethylene glycol	44.2	0.14	5.80	1.1
	water	47.7	0.15	6.03	1.1
20	air	49.1	0.52	8.01	2.2
	ethylene glycol	85.1	0.54	9.79	2.2
	water	94.6	0.57	10.23	2.2
40	air	115.1	1.98	13.57	4.4
	ethylene glycol	186.3	2.01	17.54	4.4
	water	210.5	2.07	18.26	4.4

tetradecane lubricant droplet and solution will also affect the accuracy of alignment, and are worthy to study. Fig. 6 presents the three-dimensional deformation of the tetradecane lubricant droplet in water with volume Vw of 40nl at the critical translation Δx_c=210.5μm. For clarity, the side view and top view are also displayed. To start with, the contact lines on the bottom plane of the micropart and the upper plane of the binding site coincide with the side boundaries of the micropart and binding site, and the whole areas of the micropart and binding site are wetted. As the micropart translates, however, the overlapped wetted area of the micropart and binding site decreases, and the suspended volume of the tetradecane lubricant droplet near the right-hand side of the micropart becomes larger. As a result, the contact line and wetted area on the upper plane of the binding site detached from the left-hand side and its neighborhood of the binding site. This will lead to the decrease of the computed horizontal restoring force as the micropart translates further.

4.2.2 Compression

The self-alignment of the micropart with the binding site when the micropart is subjected to compression is then investigated. As presented in Fig. 7, the dashed lines represent the computed vertical restoring force F_z versus the compression Δz in air, and the long-short dashed lines in ethylene glycol solution and the solid lines in water. Each calculation indicates that the critical vertical restoring forces occur at the critical compressions Δz_c (0.13μm, 0.52μm and 1.98μm), (0.14μm, 0.54μm and 2.01μm) and (0.15μm, 0.57μm and 2.07μm), which are at most (1.3%, 2.6% and 4.9%), (1.4%, 2.7% and 5.0%) and (1.5%, 2.9% and 5.2%) of the static height z_0 for the tetradecane lubricant droplets with various volumes in air, ethylene glycol

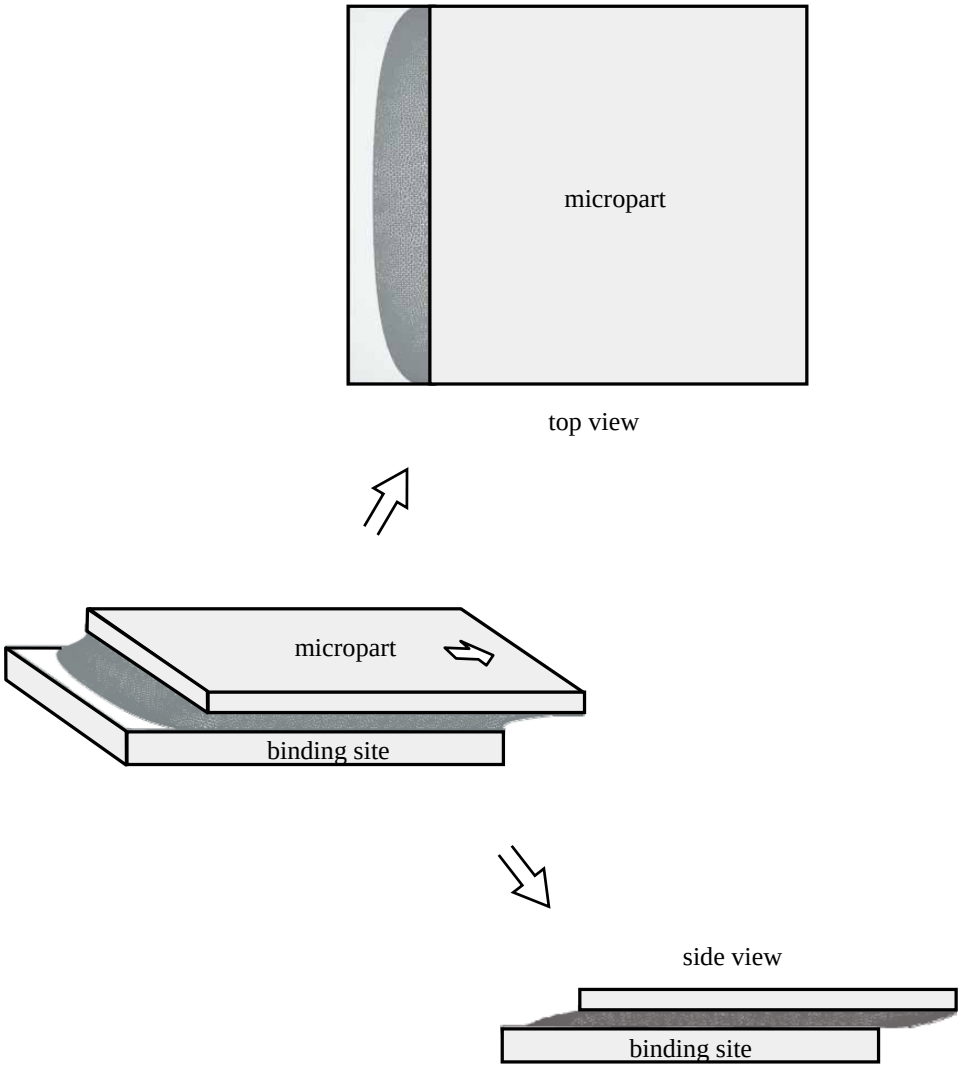

Figure 6: The three-dimensional deformation of the tetradecane lubricant droplet in water

solution and water, respectively.

As seen in Fig. 7, the vertical restoring force F_z calculated at the same volume of the tetradecane lubricant droplet in water is greater than that in ethylene glycol solution and then in air. As the compression Δz increases, the computed vertical restoring

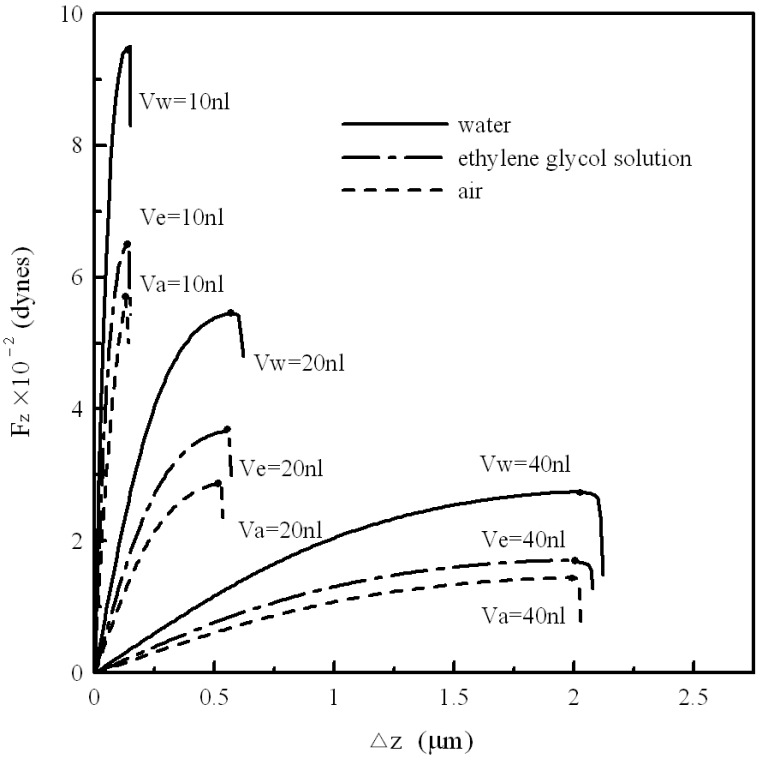

Figure 7: The computed vertical restoring force F_z versus the compression Δz of the micropart for various volumes of tetradecane lubricant droplets in different solutions

force F_z increases because the contact angle increases. The critical compression Δz_c also increases with the volume of the tetradecane lubricant droplet. When the compression Δz exceeds its critical value, the tetradecane lubricant droplet will overflow the side boundaries of the micropart, which leads a drastic drop of the vertical restoring force F_z. Consequently, the micropart cannot self-align to its initial place anymore even when the compression Δz is eliminated.

As revealed in Table 1, the critical compressions Δz_c under the same volume of the tetradecane lubricant droplet in water, ethylene glycol solution and air do not differ much, although the computed vertical restoring force F_z for the tetradecane lubricant droplet in water is still larger than that in ethylene glycol solution and air.

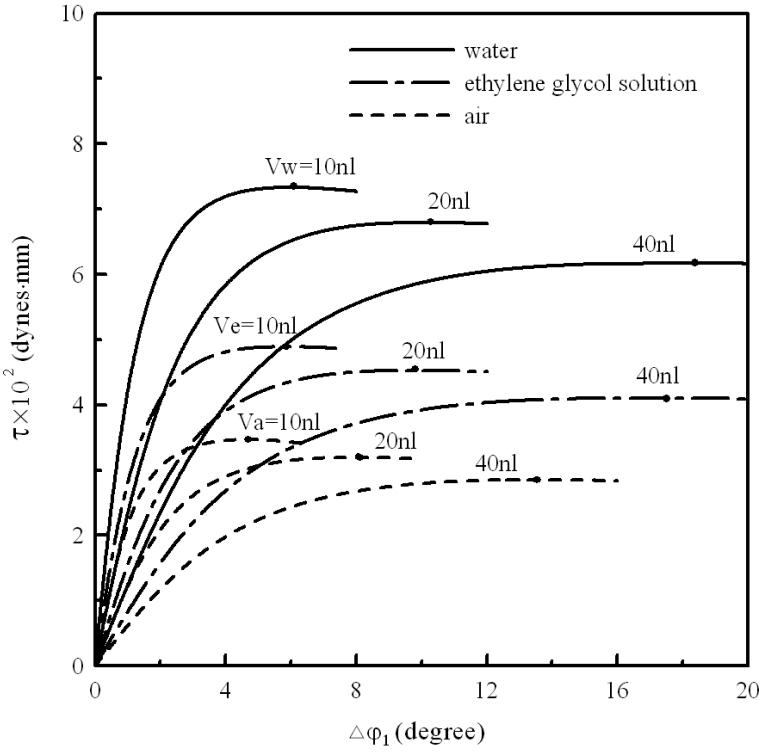

Figure 8: The computed restoring torque τ versus the yawing $\Delta\varphi_1$ of the micropart for various volumes of tetradecane lubricant droplets in different solutions

4.2.3 Yawing

This work further studies the restoring torque τ versus the yawing angle $\Delta\phi_1$ of the micropart for the tetradecane lubricant droplets with various volumes in air, ethylene glycol solution and water. As displayed in Fig. 8, the dashed, long-short dashed and solid lines represent the computed restoring torque τ under the yawing $\Delta\phi_1$ in air, ethylene glycol solution and water, respectively. The computed results show that the critical restoring torques τ occur at the critical yawing angles $\Delta\phi_{1c}$ (4.68°, 8.01° and 13.57°), (5.80°, 9.79° and 17.54°) and (6.03°, 10.23° and 18.26°), for different volumes of the tetradecane lubricant droplets in air, ethylene glycol solution and water.

As presented in Fig. 8, the critical yawing angle $\Delta\phi_{1c}$ of the micropart increases with the volume of the tetradecane lubricant droplet. As mentioned previously, the computed restoring torque τ increases with the yawing $\Delta\phi_1$, until the computed

restoring torque τ reaches its maximum. The three-dimensional deformation of the tetradecane lubricant droplet in water with volume Vw of 40nl under the critical yawing angle $\Delta\phi_1$=18.26° is demonstrated in Fig. 9. The tetradecane lubricant droplet is suspended at the corners of the micropart. When the micropart rotates over the critical yawing angle $\Delta\phi_{1c}$, the contact line will detach from four corners of the binding site and the micropart cannot self-align to its initial place while the yawing angle $\Delta\phi_1$ is withdrawn. Further, the restoring torque τ increases moderately with the yawing $\Delta\phi_1$ for greater volume of the tetradecane lubricant droplet. Again, as shown in Table 1, the critical yawing angles $\Delta\phi_{1c}$ of the micropart in water do not have much difference from those in ethylene glycol solution and air, and the critical restoring torque computed by the same volume of the tetradecane lubricant droplet in water is larger than that in ethylene glycol solution and air.

4.2.4 Rolling

The computed restoring torque τ versus the rolling angle $\Delta\phi_2$ for the tetradecane lubricant droplets with various volumes in air, ethylene glycol solution and water is analyzed finally. As displayed in Fig. 10, the dashed, long-short dashed and solid lines represent the computed restoring torque τ under the rolling angle $\Delta\phi_2$ in air, ethylene glycol solution and water, respectively. Because the static heights z_0 under the same volume of the tetradecane lubricant droplet are similar, the critical rolling angles $\Delta\phi_{2c}$ obtained in air, ethylene glycol solution and water are almost the same. As seen in Table 1, the critical rolling angles $\Delta\phi_{2c}$ increases with the volume of the tetradecane lubricant droplet. The critical restoring torques are respectively calculated at the critical rolling angles $\Delta\phi_{2c}$ 1.1°, 2.2° and 4.4° for the tetradecane lubricant droplets with different volumes in air, ethylene glycol solution and water. As the rolling angle $\Delta\phi_2$ increases, the restoring torque τ also increases until the micropart touches the binding site. The results indicate that, when the micropart hasn't touched the binding site yet, the micropart will self-align to its initial place due to its restoring torque τ as the rolling angle $\Delta\phi_2$ is removed. It is also mentioned that the restoring torque τ for the tetradecane lubricant droplet in water is greater than that in ethylene glycol solution or air.

After comparing the self-alignment of the micropart under the motions of translation, compression, yawing and rolling in air, ethylene glycol solution and water, obviously, the translation and the rolling of the micropart are two major motions that most affect the accuracy of the self-alignment of the micropart. With regard to the capability of the self-alignment of the micropart, the restoring force and the restoring torque induced on the micropart for the tetradecane lubricant droplet in water are larger than those in ethylene glycol solution and air. Therefore, the capability of the self-alignment of the micropart with the binding site in water is the

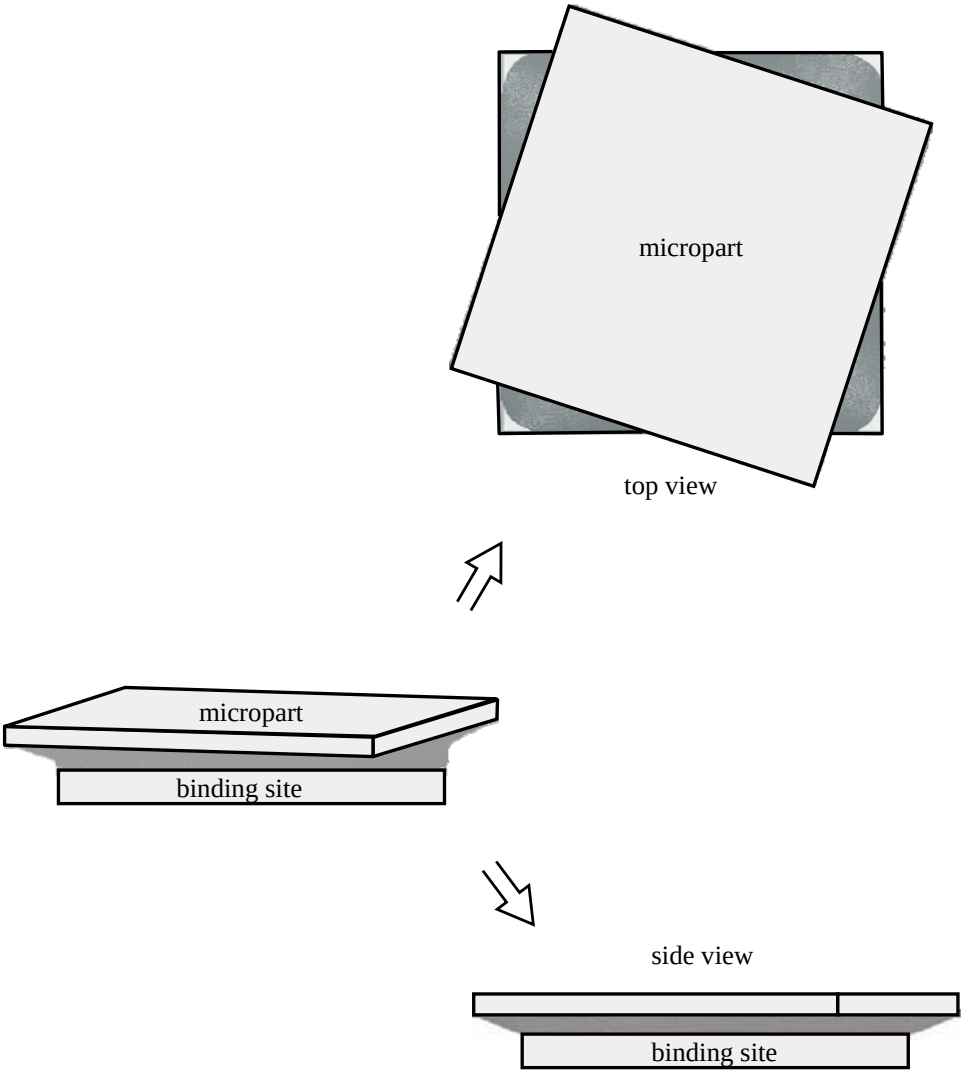

Figure 9: The three-dimensional deformation of the tetradecane lubricant droplet in water

best, the second is in ethylene glycol solution and the worst is in air.

5 Concluding Remarks

By the Surface Evolver Program, a rigorous three-dimensional analysis model has been successfully established in this work for the self-alignment of the micropart

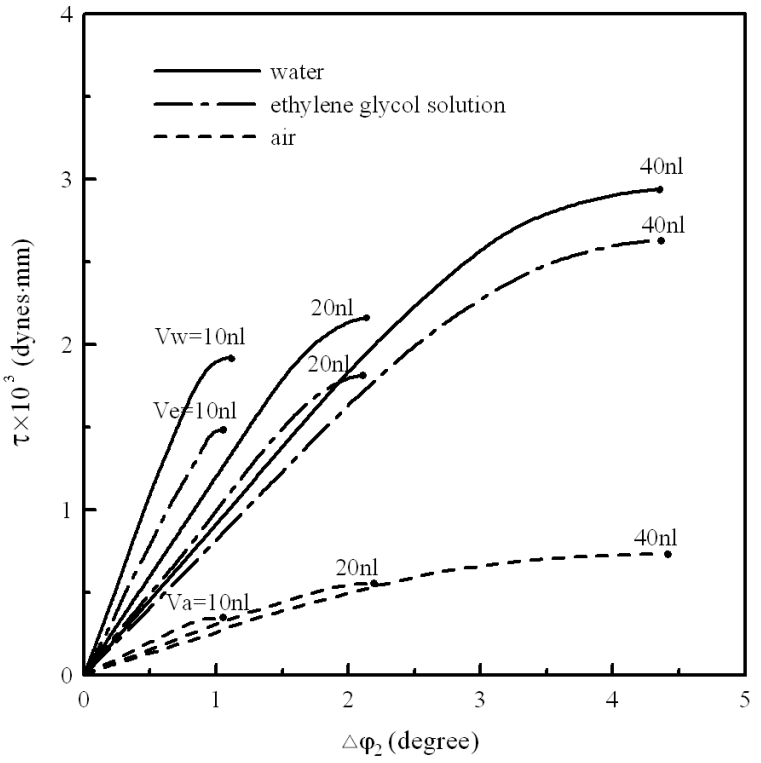

Figure 10: The computed restoring torque τ versus the yawing $\Delta\varphi_1$ of the micropart for various volumes of tetradecane lubricant droplets in different solutions

with the binding site in different solutions using various volumes of lubricant droplets. In addition to the effects of the gravity and interfacial tensions, the buoyancy and hydrostatic pressure exerted on the micropart and the hydrostatic pressure on the lubricant droplet are accurately considered in the present analysis model. The critical restoring force and restoring torque induced on the micropart, together with their critical movements, are computed under the motions of translation, compression, yawing and rolling, respectively. It is concluded that, for the self-alignment of the micropart with the binding site, the translation and the rolling are the most influenced motions and the water is the best solution as compared with ethylene glycol solution and air. Besides, based on the results achieved in this work, relevant experimental works are recommended for the future development of the fluidic self-assembly technique.

Acknowledgement: The authors are grateful to the National Science Council,

Taiwan, R.O.C., for financially supporting this research under grants NSC-98-2221-E-007-017-MY3. The authors would also like to express their thanks to Professor Ken Brakke, Susquehanna University, for his many useful discussions and suggestions for the Surface Evolver Program.

References

Berthier, J.; Brakke, K. A.; Grossi, F.; Sanchez, L.; Di Cioccio, L. (2010): Self-Alignment of Silicon Chips on Wafers: A Capillary Approach. *Journal of Applied Physics*, vol.108, no.5, pp.054905-1–10.

Böhringer, K. F.; Srinivasan, U.; Howe, R. T. (2001): Modeling of Capillary Forces and Binding Sites for Fluidic Self-Assembly. *Proceedings of the IEEE Micro Electro Mechanical Systems(MEMS)*, pp.369–374.

Brakke, K. A. (1992): The Surface Evolver. *Experimental Mathematics*, vol.1, no.2, pp.141–165.

Brakke, K. A. (1996): Surface Evolver Manual, Version 2.01. The Geometry Center. University of Minnesota.

Cabestany, J.; Rojas, I.; Joya, G. (2011): Advances in Computational Intelligence, first ed., Spring Science + Business Media, New York.

Chen, W. H.; Lin, S. R.; Chiang, K. N. (2005): Stability of Solder Bridging for Area Array Type Packaging. *CMC: Computers, Material & Continua*, vol.2, no.3, pp.151–162.

Chen, W. H.; Huang, T. Y. (2010): On the Contact Characteristics between Droplet and Microchip/Binding Site for Self-Alignment. *CMC: Computers, Materials & Continua*, vol.20, no.1, pp.63–83.

Elwenspoek, M.; Abelmann, L.; Berenschot, E.; van Honschoten, J.; Jansen, H.; Tas, N. (2010): Self-assembly of (sub-)Micron Particles into Supermaterials. *Journal of Micromechanics and Microengineering*, vol. 20, no. 6, pp.064001-1–28.

Greiner, A.; Lienemann, J.; Korvink, J. G.; Xiong, X.; Hanein, Y.; Böhringer, K. F. (2002): Capillary Forces in Micro-Fluidic Self-Assembly. *2002 International Conference on Modeling and Simulation of Microsystems - MSM 2002*, pp.198–201.

Inaba, H.; Sato, K. (1996): Measurement of Interfacial Tension between Tetradecane and Ethylene Glycol Water Solution by Means of the Pendant Drop Method. *Fluid Phase Equilibria*, vol.125, no.1-2, pp.159–168.

Karniadakis, G.; Beskok, A.; Aluru, N. (2005): Microflows and Nanoflows: Fundamentals and Simulation, first ed., Spring Science + Business Media, New York.

Kim, J. M.; Shin, Y. E.; Fujimoto, K. (2004): Dynamic Modeling for Resin Self-

Alignment Mechanism. *Microelectronics Reliability*, vol.44, no.6, pp.983–992.

Kim, J. M.; Yasuda, K.; Fujimoto, K. (2005): Resin Self-Alignment Processes for Self-Assembly Systems. *Journal of Electronic Packaging*, vol.127, no.1, pp.18–24.

Lienemann, J.; Greiner, A.; Korvink, J. G. (2002): Surface Tension Defects in Micro-Fluidic Self-Alignment. *Proceedings of the SPIE - The International Society for Optical Engineering*, vol. 4755, pp. 55–63.

Lienemann, J.; Greiner, A.; Korvink, J. G.; Xiong, X.; Hanein, Y.; Böhringer, K. F. (2003): Modelling, Simulation and Experimentation of a Promising New Packaging Technology - Parallel Fluidic Self-Assembly of Micro Devices. *Sensors Update*, Vol. 13, No.1, pp.3–43.

Lu, Y.; Xia, S.; Liu, M.; Zhang, J. (2006): Dynamic Simulation of MEMS Self-Assembly Using Capillary Force. *1st IEEE International Conference on Nano/Micro Engineered and Molecular Systems*, pp. 414–417.

Mastrangeli, M.; Valsamis, J.-B.; Van Hoof, C.; Celis, J.-P.; Lambert, P. (2010): Lateral Capillary Forces of Cylindrical Fluid Menisci: A Comprehensive Quasi-static Study. *Journal of Microelectromechanical Systems*, vol.20, no.8, pp.075041-1–13.

Mastrangeli, M.; Ruythooren, W.; Celis, J.-P.; Van Hoof, C. (2011): Challenges for Capillary Self-Assembly of Microsystems. *IEEE Transactions on Components, Packaging and Manufacturing Technology*, vol. 1, no. 1, pp.133–149.

Morris, C. J.; Parviz, B. A. (2008): Micro-scale Metal Contacts for Capillary Force-driven Self-assembly. *Journal of Micromechanics and Microengineering*, vol. 18, no. 1, pp.015022-1–10.

Neumann, W. A.; David, R.; Zuo, Y. (2011): Applied Surface Thermodynamics, second ed., Taylor & Francis Group, Northwest Washington.

Saeedi, E.; Kim, S. S.; Parviz, B. A. (2007): Self-Assembled Inorganic Micro-Display on Plastic. *20th IEEE International Conference on Micro Electro Mechanical Systems*, pp.755–758.

Sato, K.; Hata, S.; Shimokohbe, A. (1999): Self-Alignment of Microparts Using Water Surface Tension. *Proceedings of SPIE - The International Society for Optical Engineering*, vol.3892, pp.321–329.

Sato, K.; Ito, K.; Hata, S.; Shimokohbe, A. (2003): Self-Alignment of Microparts Using Liquid Surface Tension - Behavior of Micropart and Alignment Characteristics. *Precision Engineering*, vol.27, no.1, pp.42–50.

Srinivasan, U.; Howe, R. T.; Lieprriann, D. (2001): Microstructure to Substrate Self-Assembly Using Capillary Forces. *Journal of Microelectromechanical Sys-*

tems, vol.10, no.1, pp.17–24.

Takei, A.; Matsumoto K.; Shimoyama, I. (2010): Capillary Torque Caused by a Liquid Droplet Sandwiched between Two Plates. *Langmuir*, vol.26, no.4, pp.2497–2504.

Talghader, J. J. (1998): Integration of LEDs and VCSELs Using Fluidic Self-Assembly. *Proceedings of SPIE - The International Society for Optical Engineering*, vol.3286, pp.86–95.

Xie, H.; Koshizuka, S.; Oka, Y. (2007): Modeling the Wetting Effects in Droplet Impingement using Particle Method. *CMES: Computer Modeling in Engineering & Sciences*, vol. 18, no. 1, pp.1–16.

Yang, S.; Krupenkin, T. N.; Mach, P.; Chandross, E. A., (2003): Tunable and Latchable Liquid Microlens with Photopolymerizable Components. *Advanced Materials*, Vol. 15, No.11, pp. 940–943.

Zhu, Q.; Wang, G.; Luo, L. (1998): Optimization of Design and Manufacturing Parameters for Solder Joint Geometry and Self-Alignment in Flip-Chip Technology. *International Conference on Solid-State and Integrated Circuit Technology Proceedings*, pp.554–558.

Zill, D. G.; Cullen, M. R. (2000): Advanced Engineering Mathematics, second ed., Jones and Bartlett Publishers, Sudbury.